ELSEVIER

Acta Psychologica 107 (2001) 293–321

acta psychologica

www.elsevier.com/locate/actpsy

fMR-adaptation: a tool for studying the functional properties of human cortical neurons

Kalanit Grill-Spector [a,*], Rafael Malach [b]

[a] *Department of Brain and Cognitive Sciences, MIT, NE20-444, 77 Mass. Ave., Cambridge, MA 02139, USA*

[b] *Neurobiology Department, Weizmann Institute of Science, Rehovot 76100, Israel*

Received 20 March 2000; received in revised form 21 November 2000; accepted 22 November 2000

Abstract

The invariant properties of human cortical neurons cannot be studied directly by fMRI due to its limited spatial resolution. One voxel obtained from a fMRI scan contains several hundred thousands neurons. Therefore, the fMRI signal may average out a heterogeneous group of highly selective neurons. Here, we present a novel experimental paradigm for fMRI, functional magnetic resonance-adaptation (fMR-A), that enables to tag specific neuronal populations within an area and investigate their functional properties. This approach contrasts with conventional mapping methods that measure the averaged activity of a region. The application of fMR-A to study the functional properties of cortical neurons proceeds in two stages: First, the neuronal population is adapted by repeated presentation of a single stimulus. Second, some property of the stimulus is varied and the recovery from adaptation is assessed. If the signal remains adapted, it will indicate that the neurons are invariant to that attribute. However, if the fMRI signal will recover from the adapted state it would imply that the neurons are sensitive to the property that was varied. Here, an application of fMR-A for studying the invariant properties of high-order object areas (lateral occipital complex – LOC) to changes in object size, position, illumination and rotation is presented. The results show that LOC is less sensitive to changes in object size and position compared to changes of illumination and viewpoint. fMR-A can be extended to other neuronal systems in which adaptation is manifested and can be used with event-related paradigms as well. By manipulating experimental parameters and testing recovery from adaptation it should be possible to gain

* Corresponding author. Tel.: +1-617-258-5250; fax: +1-617-253-8335.
E-mail address: kalanit@psyche.mit.edu (K. Grill-Spector).

0001-6918/01/$ - see front matter
PII: S0001-6918(01)00019-1

insight into the functional properties of cortical neurons which are beyond the spatial resolution limits imposed by conventional fMRI. © 2001 Published by Elsevier Science B.V.

PsycINFO classification: 2323; 2520

Keywords: Object recognition; Human visual areas; fMR-adaptation; fMRI; Occipital cortex

1. Introduction

fMRI is a useful tool for mapping human brain regions due to its non-invasive nature and its ability to provide whole-brain coverage (see Savoy, 2001, for a general introduction to brain mapping techniques). However, the limited spatial resolution of fMRI (which is in the order of mm) places a barrier for studying the properties of individual groups of highly selective neurons if they are co-localized within the volume of a single imaged voxel. Using standard imaging methods one is measuring the overall neural activation within a voxel during the MR acquisition time. With these techniques, it is impossible to assess from the measured fMRI signal whether its source is the activity of a mixture of neuronal populations, each tuned to a different property or whether it is the outcome of the activity of a homogeneous group of neurons which share a common property. Therefore, in many cases it is difficult to infer from imaging data the functional characteristics of the underlying neurons, particularly, in higher brain areas in which the organizational principles of neurons are more complex and less investigated. Even the recent advances in mapping human cortical columns (Cheng, Waggoner, & Tanaka, 1999; Kim, Duong, & Kim, 2000; Menon, Ogawa, Strupp, & Ugurbil, 1997) may not provide a solution for understanding properties of neuronal groups which are not organized in large columnar structures.

This problem of spatial averaging may be transcended by using stimulus repetition effects. Recently, it has been reported that high-order human visual areas show a reduction in the fMR signal when presented repetitively with the same visual stimulus (Buckner et al., 1998; George et al., 1999; Henson, Shallice, & Dolan, 2000; James, Humphrey, Gati, Menon, & Goodale, 1999; Martin et al., 1995; Stern et al., 1996). A similar phenomenon was also reported for repetitively presented words (Buckner et al., 1995) and as the initial phase in procedural motor learning (Karni et al., 1995). It was suggested that this effect is correlated to visual priming (Buckner et al., 1998; Wiggs & Martin, 1998). The neuronal mechanisms underlying the repetition effect are not clear at this stage, but a straightforward interpretation is neuronal adaptation, namely, a reduction in the spiking rate of the adapted neuronal population. Shape adaptation by repetition has been documented by several studies in macaque IT neurons (Li, Miller, & Desimone, 1993; Miller, Li, & Desimone, 1991; Rolls, Baylis, Hasselmo, & Nalwa, 1989; Sobotka & Ringo, 1993). Lacking direct single-unit recordings from the human cortex, we will tentatively refer to the measured fMRI signal reduction as functional magnetic resonance adaptation (fMR-A).

The application of fMR-A to study the functional properties of cortical neurons proceeds in two stages. First, the neuronal population is adapted by a repeated presentation of a single stimulus. Second, some property of the stimulus is varied and the recovery from adaptation is assessed. If the signal remains adapted despite the change, it will indicate that the neurons are invariant to that attribute. If, however, the fMRI signal will recover from the adapted state it would imply that the neurons are sensitive to the property that was altered.

To clarify the reasoning involved consider as an example the question of viewpoint-invariance of object-recognition networks. This is a central issue of debate in the object recognition literature (for a review, see Edelman, 1998). Do voxels in higher-order brain areas contain a mixture of neuronal populations each tuned to a different object viewpoint or are neurons viewpoint-invariant, namely, is the representation object-centered? We will show that using fMR-A one can distinguish between these two hypotheses (Fig. 1). Presenting repetitively a face in the same viewpoint will result in the suppression of the activation of the neurons within the voxel that are tuned to this face in this particular viewpoint, resulting in a reduced fMR signal (Fig. 1(b)). If the neurons within the voxel are truly viewpoint-invariant (Fig. 1(c-right)), showing the object in different in-depth rotations will produce adaptation, similar to that produced by identical stimuli, since the neurons are essentially "blind" to this manipulation. If, on the other hand, the voxel contains a mixture of neuronal groups each tuned to a different optimal orientation (Fig. 1 (c-left)) then, each viewpoint will activate a new group of neurons. The neurons would not be adapted, and the result will be a strong fMRI signal, i.e., a recovery from the adapted state.

In the present review, we first characterize fMR-A in terms of its anatomical localization and duration in the human visual cortex. We then illustrate the use of fMR-A in the investigation of invariances of object representation in the lateral occipital complex (LOC) (Grill-Spector et al., 1998a; Grill-Spector, Kushnir, Edelman, Itzchak, & Malach, 1998b; Malach et al., 1995). Some of the results presented here were published previously (Grill-Spector et al., 1999).

2. Methods

The experimental setup and protocols were described in detail elsewhere (Grill-Spector et al., 1999). Here, we present a brief account of the main aspects of the experiments.

2.1. MRI-setup

Seventeen subjects were scanned in a 1.9 T scanner (whole-body, 2T-Prestige, Elscint, Haifa, Israel) equipped with a birdcage head coil. Back-projected images were viewed through a tilted mirror. Subjects fixated and performed covert naming (adaptation experiment) or one-back matching (all other experiments). In addition, we mapped in all of the subjects the borders of retinotopic visual areas using two

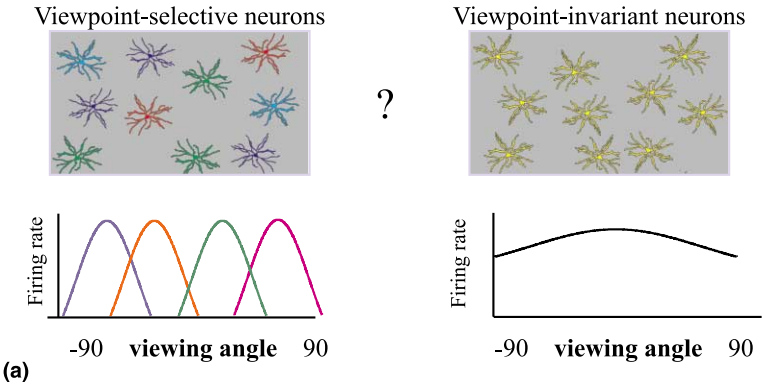
Viewpoint-selective neurons
Viewpoint-invariant neurons
?
Firing rate
Firing rate
-90 viewing angle 90
-90 viewing angle 90
(a)

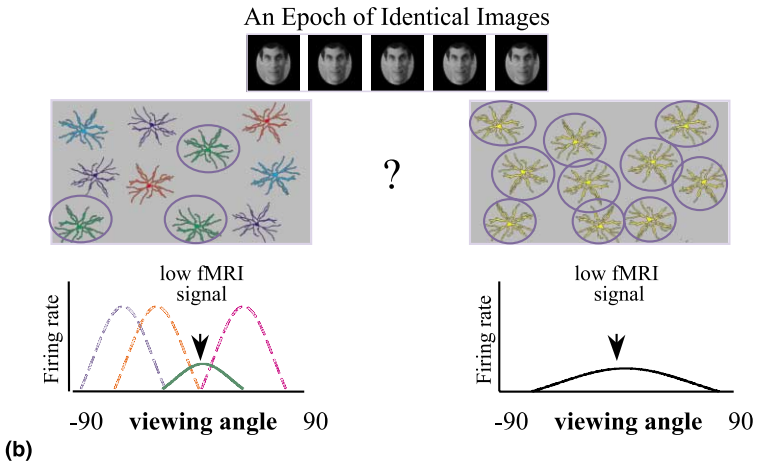
An Epoch of Identical Images
?
low fMRI signal
low fMRI signal
Firing rate
Firing rate
-90 viewing angle 90
-90 viewing angle 90
(b)

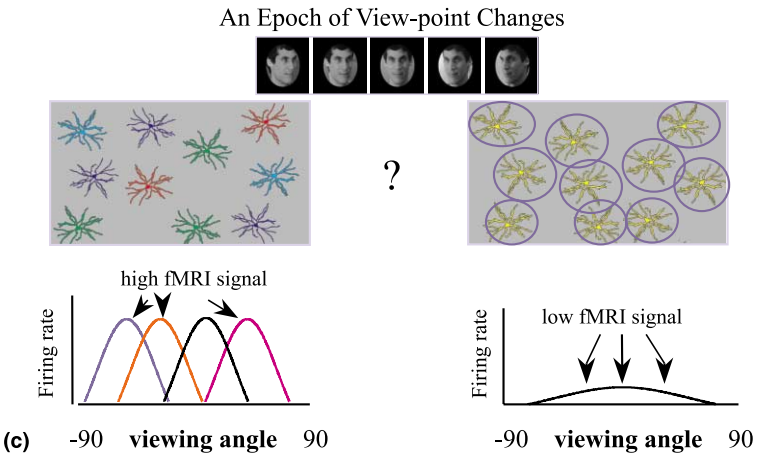
An Epoch of View-point Changes
?
high fMRI signal
low fMRI signal
Firing rate
Firing rate
(c)
-90 viewing angle 90
-90 viewing angle 90

Fig. 1. Application of fMR-A to study invariant properties of neurons. (a) The experimental question: are neurons in object selective areas viewpoint-invariant? How can we distinguish using fMRI between two alternatives: do voxels contain several populations of neurons, each tuned to a selective range of viewpoints (left) or do they contain a homogeneous population of viewpoint-invariant neurons (right)? The gray area represents a voxel, each neuronal population with common properties within the voxel is colored in the same color. Bottom graphs illustrate the activation profiles of these hypothetical neurons as a function of object viewpoint. (b) Repeated presentation of identical images: (Top) visual stimulus. (Middle) Neurons within a voxel; blue ovals indicate the population of neurons that was adapted due to repeated presentation of an identical stimulus. (Bottom) Activation profile of these neurons; dashed lines indicate neurons that were not activated by this particular image. Note that repetitions produce adaptation, hence, a reduced fMRI signal in both types of hypothetical voxels. (c) Repeated presentation of the same object undergoing a transformation. Symbols same as (b). If the voxel contains viewpoint-invariant neurons (right) they will be adapted the same way as by an identical stimulus (b-right) hence, we will measure a reduced fMRI-signal. However, if the voxel contains several populations of viewpoint-selective neurons (left), each object viewpoint will activate a different neuronal population, neither population will adapt and we will measure a high fMR-signal as in a non-adapted case. Therefore, recovery from adaptation will imply selectivity for the parameter that was varied and adaptation will indicate invariance.

vertical and two horizontal log-polar sections. For details see Grill-Spector et al. (1998b). This experiment provided an independent and reliable differentiation between the LOC and its neighboring retinotopic visual areas. Using the borders defined by the meridian maps, we were able to estimate the spatial extent of retinotopic regions depicted in Fig. 3(right). In nine subjects, we mapped eccentricity bands using concentric rings.

2.2. Adaptation experiment

This experiment (see Fig. 2) consisted of five object-containing epochs lasting 32 s alternating with 16 s mean luminance blanks, randomly oriented triangles or highly scrambled pictures. Images were gray-level photographs ($30° \times 30°$ visual angle) of objects presented for 875 ms interposed with 125 ms blanks. Object categories included: animals, faces, and man-made objects. Cycle of different objects ranged from a single object presented repeatedly for 32 times, through cycles of 2, 4 and 8 different objects, and an epoch containing 32 different objects.

2.3. Face experiment 1: size-translation-rotation invariance

The experiment contained 29 epochs of 16 images ($16.875° \times 22.5°$) presented at a rate of 1 Hz face images (see Fig. 6) alternated with scrambled or blank epochs, images were presented for 750 ms followed by 250 ms mean luminance blank. Epoch types were: (1) identical: a single face presented repeatedly; (2) translation: same face translated over 5. 625° around fixation; (3) size: same face, but changed in size over a range of $9.375° \times 14°$–$18.75° \times 28°$; (4) rotation: same face but rotated over $\pm 90°$; (5) different: 16 different faces shown in the same viewing conditions; (6) scrambled: face images randomly scrambled into blocks of 10×10 pixels. Epoch order was counterbalanced. Presentations of the same face were separated by at least 7 epochs (1 min

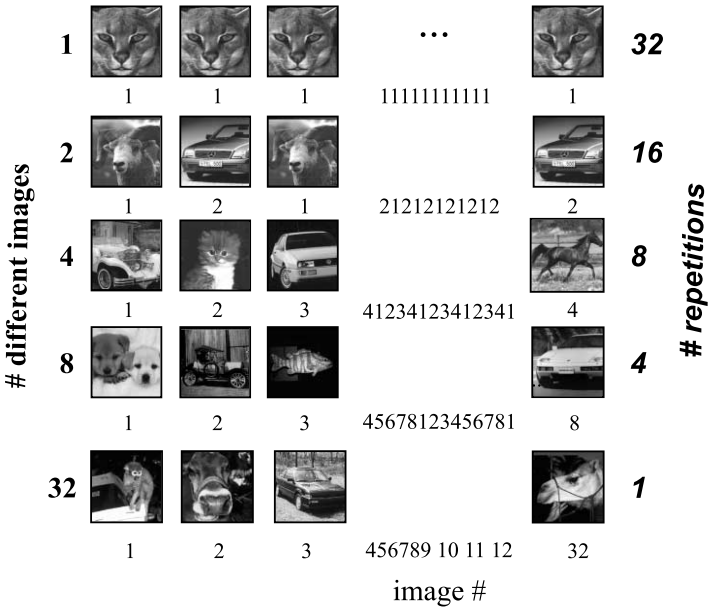

Fig. 2. The adaptation experiment. An illustration of the sequence of object images presented during the adaptation experiment (see Section 2). Each row represents an epoch. The number of different objects in each repeating cycle is given on the left, ranging from the same object-picture presented repeatedly to 32 different images. Object epochs alternated with either texture patterns, highly scrambled images or a blank field.

38 s). The occurrence of the same individual took place twice: once before the corresponding adapting (identical) epoch and once after it. Subjects were required to perform a 1-back task via a response box while fixating (same: left button, different: right button, blank: alternate buttons). Reaction times were averaged over images of a condition. Note that subjects were required to attend changes in all epochs and could not anticipate the epoch order. Thus, for most epochs the changes in the viewing conditions made the task a non-trivial one.

2.4. Face experiment 2: translation–illumination–rotation invariance

The experiment contained 32 blocks of five images presented at a rate of 0.5 Hz. Face images of size $9° \times 12°$ alternated with scrambled images or blanks. Each image was presented for 1750 ms followed by 250 ms blank. Epochs included: (1) identical (Ident.): a single face presented repeatedly; (2) translation (Trans.): same face translated over 5. 625° around fixation; (3) illumination (Illum.): same face illuminated from five different directions; (4) rotation (Rotat.): same face viewed in five rotations around the vertical axis $(-34°, -17°, 0°, 17°, 34°)$; (5) different (Diff.): five different faces; (6) scrambled: face images randomly scrambled into blocks of 10×10 pixels. Pixel-wise dissimilarity in the different epoch was the smallest (mean = 4.3)

and in the translation epoch, the largest (mean = 5.9); the dissimilarity ranking: translation > rotation > illumination > different. Each condition was repeated three times in random order using a different face. Subjects were instructed to perform a one-back matching task while fixating. Three versions of the experiment were executed (20 scans, 14 subjects) differing in epoch order and face identity.

2.5. Face and car experiment

Same as face experiments but with the addition of a second-object category: cars (see Fig. 8(a)). The experiment consisted of 45 epochs, object epochs alternated with scrambled epochs or blanks. Face and car epochs included: translation (two per category), rotation, identical and different (three per category). Presentation rate as in face experiment 2. A total of six scans were run.

2.6. Quantitative analysis of inter-picture differences

Physical picture similarity within an epoch, in each of the experiments was calculated as the mean point-wise Euclidean distance between all pairs of pictures presented in each epoch (Moses, Adini, & Ullman, 1994). Although simple, this analysis provides a baseline for comparison to more sophisticated similarity measures. Formally, the point-wise distance d_{jk}, is defined by:

$$d_{jk} = \frac{1}{n}\sqrt{\sum_{x=1}^{n}(I_j(x) - I_k(x))^2}, \quad j,k = 1 \ldots p,$$

where n is the number of pixels in an image, $I_j(x)$ is the gray-level value of the pixel in location x in the image I_j, and p is the number of images in the epoch. The mean point-wise distance (d) over all images in a condition was calculated as:

$$d = E(d_{jk})$$

and taken as the dissimilarity index. The larger this index, the greater the overall physical (i.e., retinal) dissimilarity between all the images in a particular epoch.

In all the face experiments the pixel-wise dissimilarity was smallest in epochs containing different individuals in the same viewing conditions. Thus, the fact that there was fMR-A in position and size epochs was not a trivial consequence of the retinal images being more similar than the different condition.

2.7. Data analysis

Details are presented in Grill-Spector et al. (1999). Two scans were rejected due to head motion. First four image acquisitions were discarded. Images were pre-processed using principal component analysis (Grill-Spector et al., 1998a; Reyment & Joreskog, 1993). The data were analyzed using regression analysis. Activation time courses were obtained from voxels showing highly significant ($P < 0.001$) activation. Statistical maps were spatially smoothed with a 3×3-pixel Gaussian filter with a

variance of 1 pixel; false positives were verified via a bootstrap method. Note that the conditions tested included only those defining object-related activation (e.g., different objects > noise) and did not include conditions which were part of the expected outcome, namely, the localization of object-areas was unrelated to the measured fMR-A effect.

2.8. Adaptation ratio

The adaptation ratio was defined as the ratio between the activation (percent signal change) in a condition and the activation of the different objects epoch (typically the maximal, non-adapted, epoch). The activation was measured relative to the adjacent (blank or scrambled) epochs to eliminate possible low-frequency fluctuations. A ratio of 1.0 indicates that there is no adaptation (e.g., Figs. 7 and 8).

2.9. Simulating the results of the adaptation experiment

The estimated time courses of activation in the different blocks of the adaptation experiment were simulated using a linear model (Boynton, Engel, Glover, & Heeger, 1996). We modeled the time course as a summation of the responses to individual images, the non-linearity introduced was that the amplitude of the hemodynamic response of identical images monotonically decreased with the number of image repetitions.

The fMRI signal $s(t)$ was given by:

$$s(t) = \sum_{j=1}^{n} \sum_{i=0}^{p} a(i,j)h(t - t_{i,j}),$$

where p is the number of different images in a cycle, n is the number of image repetitions; $a(i,j)$ denotes the amplitude of the jth repetition of the ith image; $h(t)$ is the ideal hemodynamic response. p was set in the different blocks to: 1, 2, 4, 8 and 32, and n was set to be 31, 15, 7, 3 and 0, respectively. The amplitude of each new image $a(i,0)$ was set to one. Thus, in the non-repeating epoch (**32**) all amplitudes were set to 1. We simulated two different models for describing the adaptation effect: a linear reduction in the amplitude: $a(i,j) = 1 - \alpha \times j$ ($0.03 < \alpha < 0.07$; see Fig. 5(c)) and an exponential reduction: $a(i,j) = \exp(-\alpha \times j)$ ($0.03 < \alpha < 0.09$; see Fig. 5(d)). The best fit for the linear model was obtained using a decay of $\alpha = 0.04$ (mean square error – MSE = 0.03), and for the exponential model: $\alpha = 0.07$ (MSE = 0.01).

The ideal hemodynamic response $h(t)$ was modeled separately using a γ function (Boynton et al., 1996; Buckner et al., 1998) or a Gaussian function (Rajapakse, Kruggel, Maisog, & von Cramon, 1998). The adaptation ratios did not depend on the function we chose to model the ideal hemodynamic response, but the overall shape of the time-course varied slightly. In Fig. 5 we present the results of the simulation based on a γ function.

3. Results

3.1. Characterizing the dynamics of fMR-adaptation

Before attempting to use fMR-A to study invariances of object-representation, it is essential to establish the magnitude, duration and anatomical localization of this effect. To that end, we performed an experiment in which object epochs included several cycles of repeating visual objects. Object epochs differed in the number of different objects presented in the repeating cycle from one object-image presented repeatedly to 32 different object-images presented once.

We analyzed separately regions activated preferentially to objects compared to textures and vice versa (for details, see Grill-Spector et al., 1999). The locations of these activation maps were compared to the representation of visual meridians that delineate borders of retinotopic areas (DeYoe, Bandettini, Neitz, Miller, & Winans, 1994; DeYoe et al., 1996; Engel, Glover, & Wandell, 1997; Engel et al., 1994; Grill-Spector et al., 1998b; Sereno et al., 1995).

Areas activated preferentially by objects lie anterior and lateral to retinotopic regions (see Fig. 3(right)), indicating that they are largely non-retinotopic, they included several distinct foci (see Fig. 3(left)): (1) the LOC which is composed of two putative subdivisions (Grill-Spector et al., 1999): (a) the posterior subdivision termed lateral occipital – LO – red in Fig. 3, located on the lateral aspect of the occipital lobe, extending into the posterior inferior-temporal sulcus; (b) the anterior-ventral part of the LOC located in the posterior to mid fusiform gyrus – posterior fusiform (pFs) – orange in Fig. 3 (Halgren et al., 1999); (2) a dorsal focus (DF) of activation was evident in 10 out of 17 subjects; (3) finally, a small region was located within the collateral sulcus (Cos – magenta in Fig. 3) medial to LOC. Cos voxels displayed object selectivity in the adaptation experiment, but not in the face experiments (see Section 2) and were selectively activated by cars in the face and car experiment.

Medial occipital areas were activated preferentially by visual noise patterns. A comparison between these maps and the borders of retinotopic visual areas as defined by the vertical and horizontal meridian mappings (see Section 2) indicated that areas preferentially activated by visual noise corresponded to areas V1–V2 with an occasional overlap with VP.

Here, we will focus on the invariant properties of object representation in lateral–ventral object-areas (LOC) that are associated with object recognition (Damasio, 1990; Damasio, Tranel, & Damasio, 1990; Grill-Spector et al., 1998a; Ungerleider & Mishkin, 1982). LOC is a large complex that can be roughly described by three vertices. Table 1 provides the Talairach coordinates (Talairach & Tournoux, 1988) of these three vertices.

The adaptation profiles of the LOC and primary visual areas revealed a markedly different behavior. Fig. 4 summarizes these differences by showing data averaged from nine subjects. Note that object-selective areas (Fig. 4(a)) showed a reduced activation when the same objects were repeated, particularly in the epochs containing only one or two objects shown recurrently (epochs **1** and **2**). The activation level in these epochs was decreased compared to the level of activation in the epoch

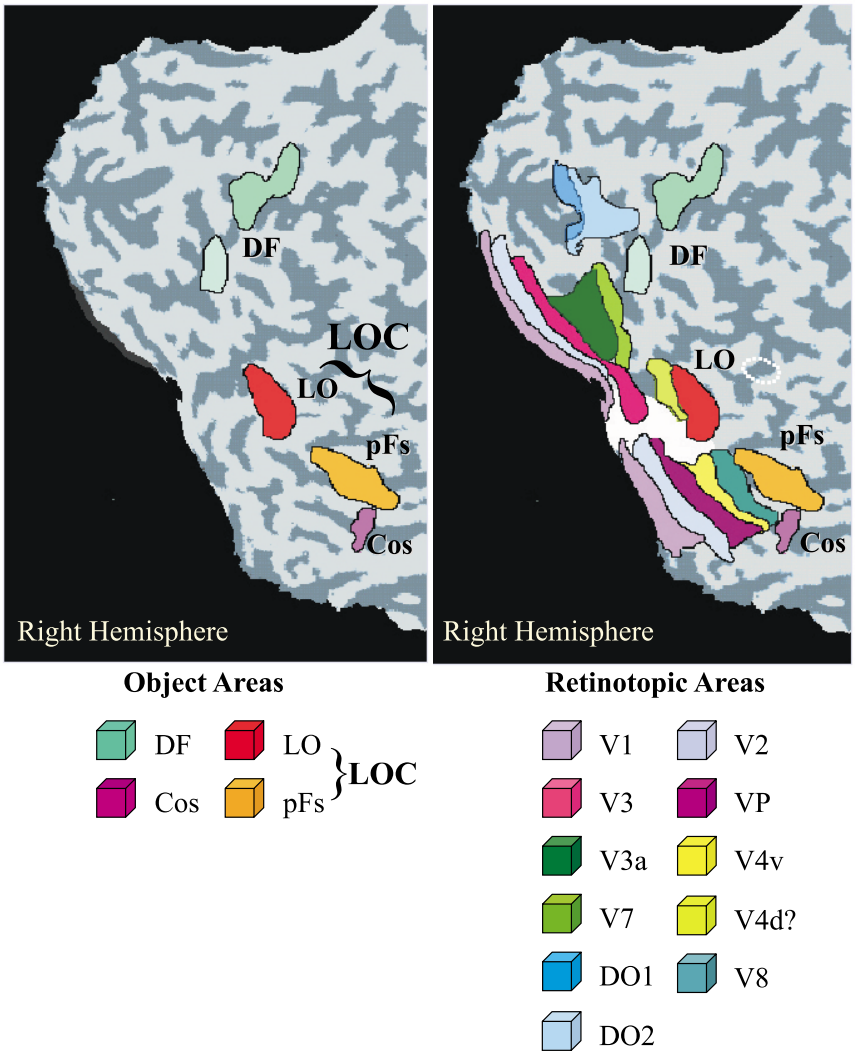

Fig. 3. Visual areas in the human cortex. The flattened map representation of visual areas in the right hemisphere of one subject was produced with the Brainvoyager software package (R. Goebel, Brain Innovation). (Left) Estimated borders of object-selective regions based on the activated areas in the different experiments presented in this paper. Regions were defined by the test (objects > scrambled) separately for each of the experiments. Abbreviations: (DF) Dorsal object selective foci located within the intra-parietal sulcus; (LOC) lateral occipital complex that was partitioned to a ventral subdivision in the posterior fusiform gyrus (pFs) and a posterior subdivision in the lateral part of the occipital lobe (LO); (Cos) collateral sulcus. (Right): Superposition of object areas and retinotopic areas. Borders of retinotopic areas were defined by the meridian mapping experiment (see Section 2). White indicates the representation of the fovea, estimated from the eccentricity experiment (see Section 2). Object selective regions fall outside of retinotopic regions and are therefore, largely non-retinotpic. DO1 and DO2 indicate dorsal regions that show some degree of retinotopy, but to our knowledge have not been named or functionally defined. V4d? represents a lower visual field representation, near but not-overlapping LO. The dashed white line indicates the estimated location of area MT.

Table 1
Talairach coordinates (Talairach & Tournoux, 1988) of four subjects who participated in the face experiments and face and car experiment[a]

	Left			Right		
	x (mm)	y (mm)	z (mm)	x (mm)	Y (mm)	z (mm)
LO	-41 ± 5	-77 ± 6	3 ± 7	40 ± 6	-72 ± 7	2 ± 5
	-36 ± 7	-71 ± 7	-13 ± 5	37 ± 5	-69 ± 7	-10 ± 4
PFs	-38 ± 5	-50 ± 6	-17 ± 5	33 ± 4	-47 ± 6	-14 ± 4

[a] They were derived from regions which showed significant preference for objects compared to noise patterns in the face and face and car experiments and were located lateral to retinotopic areas V4/V8 (Hadjikhani, Liu, Dale, Cavanagh, & Tootell, 1998). The LOC can be described by three vertices: the first row corresponds to the dorsal-posterior vertex, the second to the ventral posterior vertex and the third to the ventral anterior vertex. The first two vertices bound LO and the third vertex defined the center of pFs in Talairach space. Values represent the mean $\pm$ S.D. in mm.

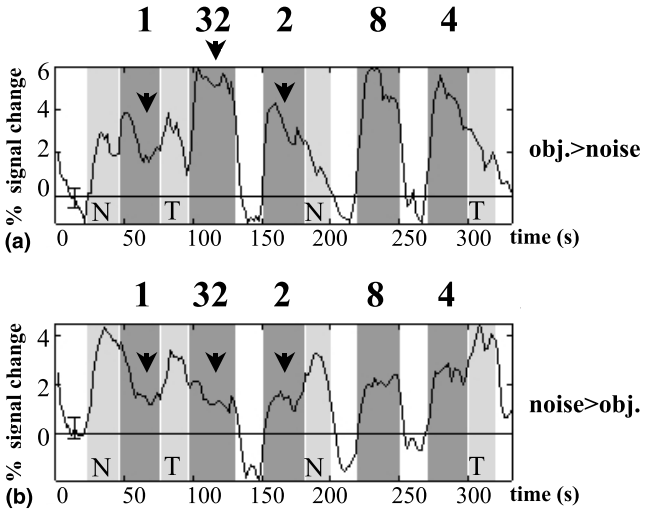

Fig. 4. Adaptation experiment: activation time courses. Averaged time course data from nine subjects. The percent signal change from a blank baseline is plotted against time. Error bars show average ± 1 standard error of the mean (SEM). Shaded regions indicate epochs in which pictures were displayed. Object epochs (see Fig. 2) are illustrated by the dark-shaded bars. Numbers on top indicate the number of different images presented in each epoch. Non-object stimuli are indicated inside the light-gray bars (T for textures and N for scrambled images). White indicates a blank field. (a) LO-complex (LOC) activation as defined by test (objects > noise and textures) and the meridian mapping experiments; (b) primary visual areas activated preferentially by visual noise compared to objects.

containing 32 different images (epoch **32**). Adaptation was rapid occurring within the first few seconds of presentation, such that the signal never attained the maximal non-adapted level of activation. Epochs containing cycles of four and eight images exhibited a more gradual reduction of signal amplitude. In contrast, primary visual

areas that showed preferential activation to visual noise patterns (Fig. 4(b)) showed similar activation levels in the different repetition cycles, i.e., these areas remained essentially un-adapted under the specific conditions of this experiment (compare epochs **1** and **2** to epoch **32**, Fig. 4(b)). The lack of adaptation in primary areas may be due to the flicker occurring when images were changed, or the use of object stimuli that are sub-optimal for the activation of primary visual areas. Although subjects maintained fixation throughout the experiment (Grill-Spector et al., 1999), considering the small receptive fields of V1 neurons, it is also possible that micro-saccades prevented the ability to provide identical retinal stimuli during the adaptation stage.

3.2. Simulating the time-courses of the adaptation experiment

The outcome of this experiment reveals that when identical images were presented repetitively, the signal in higher-level visual was reduced compared to an epoch when an equivalent number of non-repeated images was presented at the same rate. Several of the factors that may influence the depth of this adaptation include the repetition frequency, the number of intervening stimuli and the number of image repetitions. To quantify these parameters, we analyzed the relationship between the level of activation of each object epoch compared to the maximal activation (epoch **32**) by calculating reduction in the signal due to image repetitions, i.e., the adaptation ratio (see Section 2). When one object picture was shown recurrently, the signal strength in LOC was reduced at the second half of the epoch to $42 \pm 6\%$ (SEM), of the activation in the no-repetition epoch. Note that even in the eight-picture cycle (number of repetitions = 7) there was a slight decrement in signal strength ($92 \pm 5\%$). As depicted in Fig. 5(a) the fMR amplitude decreased monotonically as the number of repetitions increased. We quantified the relationship between the signal reduction both as a function of the total number of image repetitions in a block (blue in Fig. 5(a)) and as a function of the number of repetitions in a time window of 16 s – which is the duration of the hemodynamic response (red in Fig. 5(a)).

We simulated the responses in the different epochs of the adaptation experiment using an almost linear summation model (see Section 2 for details) of ideal hemodynamic responses as depicted in Fig. 5(b). Instead of summing hemodynamic responses with a constant amplitude, the amplitude of hemodynamic responses of repeated images was set to be decreasing, as a function of the number of image recurrences. Non-repeating images were treated independently. Thus, the estimated response in block (**32**) containing 32 non-repeating images (see also, red graph in Figs. 5(c) and (d)) was the summation of the individual hemodynamic responses of all images with a constant amplitude of 1.0. The response in block (**1**) of one image presented repeatedly was a summation of hemodynamic responses with progressively decreasing amplitudes due to adaptation. Blocks containing several cycles of repeating images (**2**, **4**, **8**) were simulated similarly. For example, in the eight-picture block, in the first cycle we summed eight shifted hemodynamic responses with an amplitude of 1.0, in the second, we summed again eight responses but with a smaller amplitude, and so forth for the rest three repetitions. We used two models in the simulation: a linear decrease in the amplitude (Fig. 5(c)) and an exponential decrease

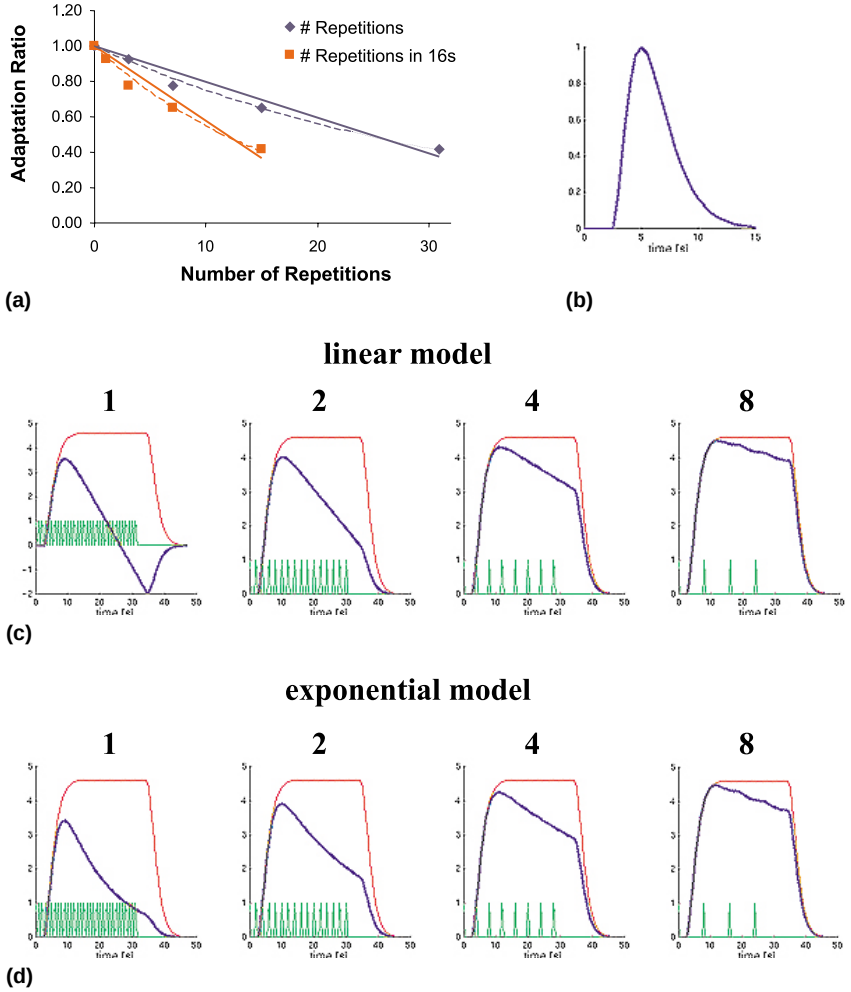

Fig. 5. Simulating the adaptation experiment time courses with an almost linear model. (a) Adaptation ratio as a function of image repetitions, *X*-axis: number of image repetitions; *Y*-axis: adaptation ratio compared to the maximum, i.e., the epoch in which 32 non-repeated images were presented. Solid lines indicate a linear trend-line and dashed lines denote an exponential fit. Exponential curves provide a slightly better fit. Note that adaptation increases (smaller ratio) with an increasing number of image repetitions. (b) An ideal hemodynamic response: γ function (Boynton et al., 1996) with parameters (Buckner et al., 1998): $\delta = 2.5$ s $\tau = 1.25$ s and an arbitrary maximum at 1.0. This model was used for estimating the response in the different epochs. (c) c and d. The estimated hemodynamic response (blue) for each of the epoch types denoted by numbers on top. Red: Estimated response in the **32** epoch, in which 32 non-repeated images were presented – in the simulation of this epoch images were treated independently, each one evoked a hemodynamic response with an amplitude of 1. Green: illustration of the times in which an identical image was presented in the different epoch types. Note that in epochs **2**, **4** and **8** we presented several cycles of repeated images (see Fig. 2). However, for clarity only one is displayed in the figure. (c) The estimated time-course in different blocks using a linear reduction in the amplitude of the hemodynamic response of repeated images ($\alpha = 0.05$). (d) The estimated time-courses using an exponential model for the decrease ($\alpha = 0.07$).

(Fig. 5(d)) using a range of parameters derived from Fig. 5(a). Qualitative comparison between the simulation results (Fig. 5(c) and (d)) and the measured signal (Fig. 4(a)) suggests that the signal decrement due to repetitions is not a linear function of image repetition, since the linear models predicts a negative signal in the identical epoch (see Fig. 5(c- far left)) that was not observed. The shape of the time-course using an exponential decrease is more consistent with the shape of the measured signal (compare to Fig. 4(a)). Thus, adaptation can be described as non-linear, monotonic reduction due to image repetitions (see Section 4.1 for further discussion). It still remains to be verified whether an exponential model is the best fit.

The outcome of the simulation suggests that the response profile of the adaptation experiment can be described using an almost linear model. The only non-linearity introduced here was the decrease in the amplitude of hemodynamic responses of recurring images. This model is consistent with the fact that the signal never attained the maximum in epochs when only 1 or 2 images were shown repetitively and also correlates with the monotonic decrease of the signal during epochs in which four or eight images cycled through the epoch.

3.3. Comparison of object transformations

The demonstration that fMR-A is a consistent and robust effect, makes it a potentially powerful tool to dissect the functional properties of neuronal groups at a sub-voxel spatial scale. Here, we illustrate the use of fMR-A to study the ability of neurons in higher-order object-related areas to generalize (be invariant) across changes in retinal position, illumination, object size and in-depth rotation. Activation to identical objects undergoing these changes was compared to different objects in the same viewing conditions (e.g., Fig. 6). We analyzed separately the two subdivisions of the LOC: the more anterior-ventral subdivision (pFs) and the dorsal-posterior subdivision LO (see Fig. 3).

Attention and ordering effects were controlled. Subjects were instructed to perform a 1-back recognition task while fixating, namely, to notice whether consecutive images belong to the same individual or to different individuals. Each condition was repeated two to three times in random order, using different images (see Section 2).

3.4. Face experiment 1: size–translation–rotation invariance

In this experiment, performed on nine subjects, we examined the effects of three transformations: size, translation and rotation, using faces as the object class (see Fig. 6). LOC was defined by a statistical test that searched for voxels activated preferentially by different faces compared to highly scrambled images (different $>$ scrambled, other conditions ignored). Time courses and adaptation ratios were extracted separately for the two subdivisions LO and pFs (see Fig. 7(a)). Both regions were adapted by repeated presentation of identical images. However, the results revealed a differential adaptation profile in the LOC. The posterior region (LO – Fig. 7(a)) showed substantial recovery from adaptation induced by size, translation and rotation. In the anterior-ventral part (pFs – Fig. 7(a)), there was a

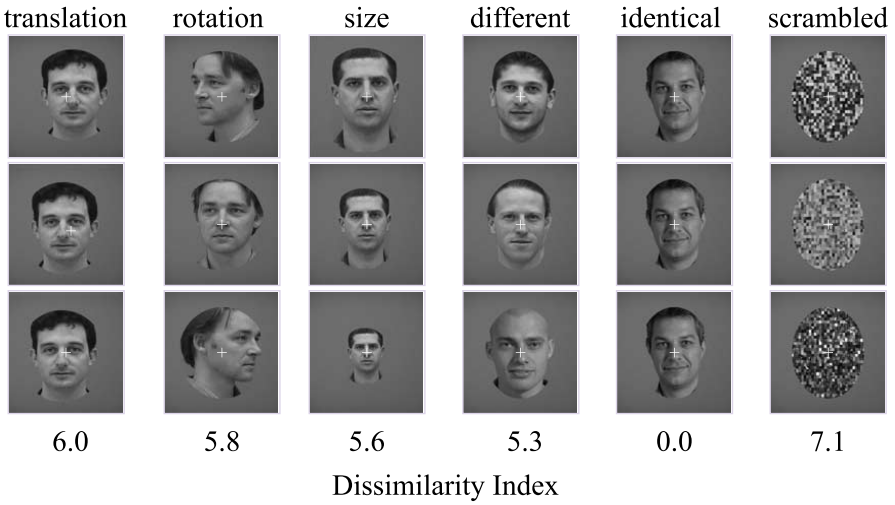

Fig. 6. Face experiment 1: size–translation–rotation invariance. Examples of images presented in the various conditions are shown in columns (see Section 2). Object epochs alternated with 10 s scrambled or blanks trials. (translation) Same face translated in the image plane; (size) the same face in different sizes; (rotation) same face rotated around vertical axis; (different) individuals shown in the same viewing conditions. (identical) repetitions of an identical face; (scrambled) Highly scrambled faces. Numbers indicate the average retinal dissimilarity between images in an epoch (see Section 2). Pixel-wise dissimilarity ranking was: translation > rotation > size > different.

marked difference between viewing conditions with strongest adaptation during position and size changes and only slight adaptation for rotations of the same face. To evaluate the differential nature of adaptation within pFs, i.e., the stronger adaptation by translation and size compared to rotation, we calculated for each subject the following activation ratios: translation/rotation and size/rotation. We then tested whether these ratios were significantly smaller than 1.0. The results for both ratios were significant (translation/rotation < 1.0, $P < 0.01$, $n = 9$; size/rotation < 1.0, $P < 0.04$, $n = 9$).

3.5. Face experiment 2: translation–illumination–rotation invariance

In this experiment, performed on 14 subjects we examined three invariances: translation, illumination and rotation using again faces as the object category. The results of the separate analysis of the two subdivisions are shown in Fig. 7(b). Both regions were maximally activated by images of different individuals (Diff. in Fig. 7(b)) and were adapted by repeated presentation of identical images (Ident. in Fig. 7(b)). However, there was a difference between the two subdivisions in their recovery from adaptation, mainly in the object-translation epochs: LO voxels exhibited substantial recovery from adaptation (ratio $= 0.94 \pm 0.17$), while pFs voxels showed only partial recovery under object translation (ratio $= 0.74 \pm 0.08$). Interestingly, even pFs voxels that exhibited the highest degree of adaptation recovered

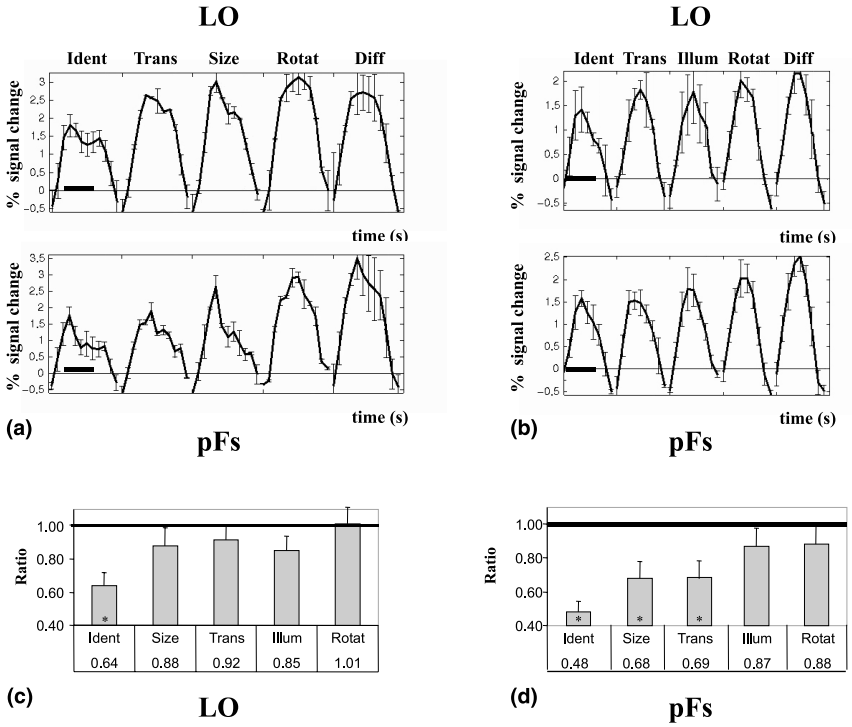

Fig. 7. Face experiments: time courses and ratios. (a) Face experiment 1: time courses taken separately from LO and pFs and averaged across nine subjects. Recurrences of the same condition were averaged; error bars indicate the standard deviation of a condition. Percent signal change was measured from the adjacent epochs. The dark horizontal bar = 10 s. Red vertical line indicates the termination of the visual stimulation in an epoch. Abbreviations correspond to epochs shown in Fig. 6. (b) Face experiment 2: time courses taken separately from LO and pFs averaged across 14 subjects and 20 scans (three versions of the experiment, see Section 2). Conventions and abbreviations same as above. (c) and (d) Face experiments adaptation ratios calculated as the mean signal in an epoch divided by the mean signal in the different epoch (see Section 2). A ratio of 1.0 indicates no adaptation. Ratios that were significantly less than 1.0 are marked by asterisks. Error bars indicated one standard error of the mean (SEM). Note the difference between LO and pFs ratios especially in the translation and size epochs.

from adaptation when the viewpoint or the direction of illumination of the same face changed. The differential profile of adaptation was statistically significant (translation/rotation < 1.0, $P < 0.03$, $n = 14$; translation/illumination < 1.0, $P < 0.02$, $n = 14$).

To summarize the effects of the different transformations, we calculated the adaptation ratios for all object transformations and subjects in the face-experiments for the two subdivisions of the LOC (see Fig. 7(c)). Note the differential adaptation effect in the pFs: while this region was adapted by size and position changes, it recovered from adaptation when the illumination direction or object pose was varied. In LO, all transformations caused a higher-level of recovery from adaptation compared to pFs.

3.6. Face and car experiment

It could be argued that the adaptation effects revealed in the face experiments are unique to this category, since faces are widely considered as a special class of objects (Farah, Klein, & Levinson, 1995; Farah, Wilson, Drain, & Tanaka, 1998; Kanwisher, McDermott, & Chun, 1997; see also De Gelder & Rouw, 2001). To examine this issue, we conducted a face and car experiment, which compared in six subjects, the fMR-A effect for two object categories, faces and cars, under two image transformations, rotations and translations. As in the face experiments, we found differential fMR-A for the different transformations both for faces and cars. The activation profiles and the adaptation ratios are shown in Figs. 8(b) and (c) for LO and in Figs. 8(d) and (e) for pFs. In both subdivisions, the absolute level of the fMR signal was higher for faces compared to cars (see Figs. 8(b) and (d)) although faces and cars were given the same weight in the statistical test. Interestingly, despite this difference, the level of fMR-A was similar for faces (light gray in Figs. 8(c) and (e)) and cars (dark gray in Figs. 8(c) and (e)). Both in LO and pFs rotations caused a recovery from adaptation, i.e., an elevated signal compared to epochs of identical images. However, in this experiment, a smaller degree of recovery from adaptation was detected in LO in the face-translation epochs. The significance of the differential profile of the fMR-A was verified (translations/rotations < 1.0, $P < 0.01$, $n = 6$, both object classes).

4. Discussion

4.1. Parameters affecting fMR-adaptation

The fMR-A described in this study was a consistent phenomenon that appeared in all subjects and under a variety of stimulus conditions. Adaptation was typically rapid, so that the fMR signal never attained the non-adapted level. Additionally, a more gradual reduction in signal amplitude was also observed, particularly, in cases of partial adaptation (e.g., Fig. 4(a) epochs **2** and **4**, and Fig. 6(a)). fMR-A was strongest when an identical object image was repeatedly presented for an extended period. However, the magnitude of the effect varied between experiments, suggesting that additional factors modulated the strength of the adaptation effect. Likely, factors were the number of repeated presentations, the repetition frequency, the type of stimuli, the order of the different epochs and top–down effects.

The effect of repetition number on adaptation level was quantified across all experiments by calculating the adaptation ratio in LOC in the identical epoch compared to the non-repeated epochs. The rate of image presentation varied between experiments, although both identical and non-repeated images in each experiment were presented at the same frequency. It is evident from Fig. 9(a) that fMR-A increases gradually (smaller adaptation ratio) as the number of repetitions increases. However, the graph suggests that the first several repetitions produce a more substantial reduction in the signal strength compared to later repetitions. Also the

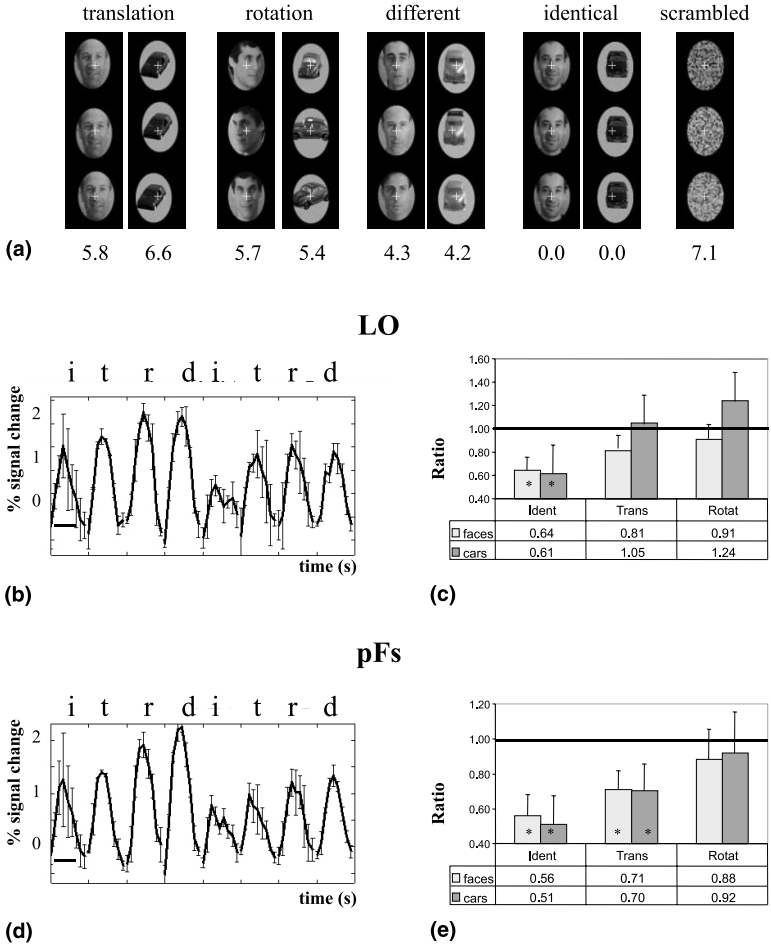

Fig. 8. Face and car experiment. (a) Examples of images presented in the various conditions are shown in columns (see Section 2). (translation) Five instances of the same object translated in the image plane; (rotation) five views of the same object; (different) five different exemplars of a category in the same viewing conditions; (identical) five repetitions of an identical image; (scrambled) five highly scrambled object images. Numbers at bottom indicate the average dissimilarity between images in a condition (see Section 2). Pixel-wise dissimilarity ranking was: translation > rotation > different. (b)–(d) Time course and adaptation ratios of LOC voxels activated preferentially by objects (faces & cars > scrambled). The LOC was subdivided into LO and pFs using meridian mapping and anatomical criteria: (b) LO time course ($n = 6$); conventions same as Fig. 7(b). Abbreviations: i = identical; t = translation; r = rotation; d = different; (c) the adaptation ratio of LO voxels (same conventions as in Fig. 7(c)). Ratios were calculated separately for faces and cars. Asterisks indicate significant reduction; (d) pFs time course ($n = 6$) same conventions as in (b); (e) The adaptation ratio of pFs voxels, same conventions as in (c).

simulation of time courses of the adaptation experiment (Fig. 5) indicates that the amount of reduction of the fMR signal by each image recurrence is monotonically decreasing, but not at a constant rate.

We also calculated the relationship between the fMR-A effect and the repetition frequency (see Fig. 9(b)). Again, the fMR signal decreased as the repetition frequency increased. This suggests that if repeated images are presented at lower frequencies, adaptation should be smaller. We cannot estimate based on the present data the extent of adaptation when images are separated more than 8 s apart. It is possible that at longer lags the response returns to its non-adapted amplitude. However, several reports suggest that effects of signal reduction for previously seen images might be long lasting (Buckner et al., 1998). In the adaptation experiment both the temporal separation between recurring images and the number of repeated pictures were changed concurrently. Consequently, we cannot separate the effects of image lag from the effects of the number of image repetitions in that experiment.

Two recent event-related studies have investigated the effect of number of repetitions and stimulus lag (Henson et al., 2000; Jiang, Haxby, Martin, Ungerleider, & Parasuraman, 2000) on the amplitude of the fMR signal. Both studies show that regions within the fusiform gyrus show a progressive signal decrease with the number of repetitions, but if repetitions are separated by a long duration the fMR signal resets back to a higher amplitude. Contrary to our study and others (Buckner et al., 1998; Jiang et al., 2000; Martin et al., 1995; Stern et al., 1996), Henson et al. (2000) claim that fMR-A in the fusiform gyrus is evident only for familiar faces or symbols, and the opposite effect (i.e., a signal increase) occurs with unfamiliar faces or symbols. The source of this difference is unclear. It may reflect heterogeneity within the pFs and associated areas. However, it should be emphasized that the different adaptation studies vary in their experimental paradigms. Therefore, further research is required to elucidate the factors that influence fMR-A, whether it is the number of repetitions, their temporal separation, the number of intervening stimuli or the task.

The temporal dynamics of neurons in higher-level visual areas in humans are still unknown, but they can be investigated using ERP measurements (Rugg, Soardi, & Doyle, 1995). A recent study (Puce, Allison, & McCarthy, 1999) of face-specific

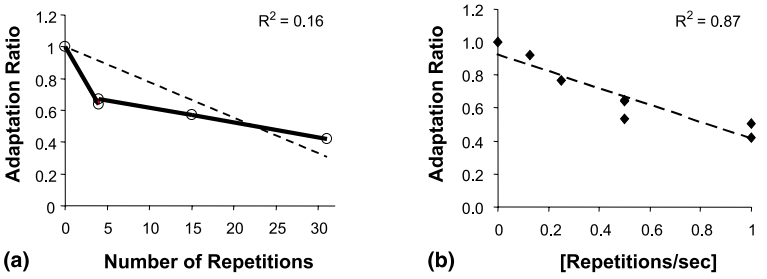

Fig. 9. Parameters that affect the strength of the fMR-A effect. (a) The adaptation ratio in identical epochs taken from the different experiments as a function of number of image repetitions. Note that as the number of repetition increases the adaptation increases (smaller ratio). However, the graph implies that the first several repetitions produce higher adaptation compared to later repetitions. Dashed line denotes the linear trend-line, although the linear fit is poor. (b) The adaptation ratio as a function of repetition frequency. Dashed line denotes the linear trend-line.

ERPs employing intra-cranial recording from patients before they underwent surgery for epilepsy, showed that late face-specific responses (N700) showed effects of amplitude reduction due to repeated repetitions of the same face. Different from monkey studies (Li et al., 1993) earlier face-specific responses (N200) showed only a decrease due to the second presentation but not a progressive decrease in signal amplitude. Thus, it remains to be established if the source of fMR-A is a local, prompt and automatic effect, or whether it is also influenced by slower top–down processes.

4.2. Neuronal mechanisms underlying the adaptation effect

A straightforward neuronal explanation for the fMR-A effect is a reduction in neuronal spiking activity. Neuronal adaptation effects were found in monkey IT where repeated presentation of the same stimulus resulted in a decreased activation of neurons, a phenomenon termed adaptive mnemonic filtering (Miller et al., 1991). This effect has interesting parallels with the fMR-A reported here, in particular a gradual increase of adaptation level with increased number of image repetitions (Li et al., 1993).

However, at this stage other potential sources for adaptation-like effects in the fMR signal cannot be excluded. One alternative may be that in the non-adapting epochs, distinct neuronal groups selective for different shapes were sequentially activated, while in the adaptation epochs only a single population of shape-selective neurons was continuously activated. If the activation of the neurons or their effect on the hemodynamic response lasted beyond the termination of the optimal stimulus for a neuronal group, an accumulation of activation causing a gradual build-up of the fMR signal could have occurred in the non-adapting epochs compared to the identical epochs, leading to a reduced measured signal in the identical epochs. However, there are several new results that argue against a build-up mechanism as an explanation of the fMR-A effect: (1) In a recent study using a masking paradigm (Grill-Spector, Kushnir, Hendler, & Malach, 2000), we have shown that the fMR amplitude by image of objects shown for 120 ms followed by a 380 ms mask was 91± 2% of the activation elicited by objects presented for 500 ms. This suggests that about 90% of the neuronal activation occurred during the first 120 ms, and therefore, contributions from later times or times after the stimulus was shut off are probably negligible; (2) a recent study (Kourtzi & Kanwisher, 2000) reported fMR-adaption using an event-related paradigm in which a build-up mechanism is highly unlikely.

It is important to clarify that the manifestation of the invariant properties of neurons in higher-order visual areas is not dependent on whether the underlying phenomenon is neuronal adaptation or recruitment of additional neuronal groups. If a decreased fMR signal is measured in epochs in which an object underwent a change, similar to epochs in which the same image was repeated, it suggests that neurons were activated similarly by identical and transformed images. Thus, either of these alternatives would indicate that the neurons were invariant to the changed attribute.

4.3. fMR-adaptation and repetition priming

The adaptation paradigm used here has parallels with the phenomenon of visual priming in which repeated presentation of visual stimuli changes the subject's performance (Schacter & Buckner, 1998; Wiggs & Martin, 1998). Some behavioral priming studies show size and position invariance (Cooper, Biederman, & Hummel, 1992; Fiser & Biederman, 1995; Wiggs & Martin, 1998). In others, the invariance is incomplete (Dill & Edelman, 1997). Combined behavioral and fMR event-related studies (Buckner et al., 1998; Jiang et al., 2000) demonstrate that repeated presentation of identical images facilitates performance on these images, concomitant with a reduction of the fMR signal in higher visual areas. This apparent correlation was taken as a proof that the adaptation effect is the neuronal correlate of perceptual priming (Schacter & Buckner, 1998). It has been argued that attenuated responses occur when the same processes are performed on repeated exposures, only faster or more efficiently, possibly reflecting a smaller but more selective population of activated neurons (Desimone, 1996). This might be reflected in a decrease in the mean firing of a neuronal population, and hence, a decreased fMR signal.

Only few studies have attempted to provide a direct, quantitative, correlation between behavioral priming and fMR-A. Interestingly, the few studies that performed such correlations, reveal a rather complex relationship. For example, Grill-Spector et al. (2000), reported that subliminal priming in a backward masking paradigm is actually associated with fMR signal *enhancement* rather than decrease, despite a robust behavioral priming effect. Bar, Schacher, Dale, and Tootell (1999) found a similar effect using an event-related paradigm. Henson et al. (2000) have reported both an enhancement and a reduction of fMR signal associated with priming depending on stimulus familiarity. These studies certainly make it hard to equate fMR-A with behavioral priming.

Here, we measured the reaction times (RT) of subjects in face experiment 1, when they performed a 1-back task. The mean RT for identical images was 384 ± 84 ms ($n = 9$), compared to 435 ± 64 ms in epochs containing images of different individuals. Interestingly, the RT for the same face undergoing transformations was similar to the identical condition (position: 367 ± 66, size: 335 ± 64, and rotation: 343 ± 72). Thus, on the behavioral level there was a similar level of invariance to all image transformations, at least as revealed by the shorter RT compared to the different condition. However, the adaptation effects in the various conditions were different. In particular, there was a recovery from adaptation when different views of the same object were shown. The lack of correlation between behavioral invariance and invariance in the representation in object areas implies that at least in the conditions tested in the present experiments the relationship between repetition priming and adaptation is not a simple one-to-one correspondence.

An alternative to the interpretation of fMR-A as a manifestation of priming – i.e., a type of perceptual learning mechanism, puts it in the context of filtering temporally redundant information. Such temporal high-pass mechanisms, serve an important function in focusing neuronal resources on novel visual stimuli. Adaptation effects can be found even at the retinal level (e.g., Werblin, 1973) and more recently were

found in the responses of V1 neurons to sustained contrast (Ohzawa, Sclar, & Freeman, 1985) as well as shape (Muller, Metha, Krauskopf, & Lennie, 1999). This adaptation effect is stimulus selective and robust, its time course is rapid, occurring within less than a second, and can last for several seconds. Such dynamics fits well the rapid adaptation observed in fMRI studies (e.g., Kourtzi & Kanwisher, 2000).

4.4. Invariant properties of object representation revealed by fMR-A

An expected consequence stemming from the ability of fMR-A to "tag" specific neuronal groups within a mixed population is that it will reveal subtle functional and anatomical details that are difficult to observe using conventional BOLD measurements. Here, fMR-A revealed that different image transformations which otherwise produce equal BOLD activation resulted in different levels of adaptation. In pFs, the adaptation was more invariant to size and position compared to illumination and viewpoint. A similar trend was also observed in LO, although it was quantitatively weaker. These results are in line with the reports of translation and size invariance in macaque IT by several research groups (Gross, Rocha, & Bender, 1972; Ito, Tamura, Fujita, & Tanaka, 1995). Indeed, Lueschow, Miller, and Desimone (1994) have used the neuronal adaptation phenomenon to quantify size and translation invariance of IT neurons. These neuronal invariances should be contrasted with the high degree of shape selectivity in LOC revealed by the relative lack of adaptation in the different-shaped objects epochs. The differential adaptation profile in LOC sub-regions is also incompatible with a global, non-specific arousal being the source of the fMR-A effect.

Two points should be considered when interpreting the results of fMR-A. First, the level of adaptation is always measured relatively to a maximum, presumably a non-adapted state. In our experiments, these were typically conditions in which different exemplars within an object category were presented. However, we cannot rule out the possibility that some adaptation did occur even in these presumably "non-adapting" epochs. For example, if there were common features among the different object exemplars used in the non-adapting conditions, these may have adapted neurons specifically tuned to such repeating features. Thus, conclusions that can be derived from adaptation studies refer only to the *relative* effects exerted by one set of images compared to another. Second, the adaptation effect reflects the overall changes in activity of a very large neuronal population; consequently, it may mask opposite effects that may occur within a smaller neuronal population intermixed within the larger population. For example, one could envision that a small subset of neurons in LOC is invariant to face viewpoint, and shows strong adaptation when faces are rotated; however, this adaptation is masked by a larger, viewpoint-sensitive neuronal population – leading to the impression of overall viewpoint-sensitivity. (For an overview, see also Op de Beeck, Wagemans, & Vogels, 2001.)

Keeping these cautionary points in mind, one can still make educated hypotheses regarding the profile of adaptation in high-order object areas. Different theories of object recognition suggest different substrates for the representation of objects in higher-order visual areas. Some theories (e.g., Biederman, 1987) suggest a 3D object-

centered representation, while other theories suggest a viewer centered framework, such that 2D views of an object span its representation (e.g., Edelman & Duvdevani-Bar, 1997; Poggio & Edelman, 1990; Ullman, 1996). Physiological studies in macaque IT provide evidence both for viewpoint-specific neurons (Logothetis, Pauls, & Poggio, 1995; Perrett et al., 1985; Wang, Tanaka, & Tanifuji, 1996) and viewpoint-invariant neurons (Booth & Rolls, 1998; Hasselmo, Rolls, Baylis, & Nalwa, 1989). Using conventional BOLD imaging, previous fMRI studies reported a similar fMR signal for different face viewpoints (Kanwisher et al., 1997) implying viewpoint-invariant representation of faces in the fusiform gyrus. However, as described in the introduction and illustrated in Fig. 1, conventional methods cannot distinguish between voxels containing viewpoint-invariant neurons and voxels containing a mixture of neuronal populations tuned to specific ranges of views. The use of fMR-A enabled us to investigate the properties of individual neuronal populations within the measured voxels. Thus, using fMR-A, we demonstrated that the overall activation of pFs is sensitive to different views of the same objects (faces and cars) and even voxels that showed the highest degree of face-selectivity recovered from adaptation when the same face was rotated. This indicates that the representation of a face, at least at the level of the majority of pFs neurons, is not viewpoint-invariant, arguing against a full 3D object-centered representation as proposed by some theories.

One surprising result was that viewing the same object under different directions of illumination resulted in substantial recovery from adaptation. Several models suggest that extraction of illumination could be done by lower visual areas (Lehky & Sejnowski, 1988). Our results suggest that sensitivity to the direction of illumination is retained even in higher levels of the visual hierarchy. While size and position changes are probably compensated for in pFs, illumination is not. These results are in line with the reported sensitivity of IT neurons to stimulus shading (Ito, Fujita, Tamura, & Tanaka, 1994). Recent psychophysical experiments (Tarr, Kersten, & Bülthoff, 1998) demonstrate the importance of illumination in object recognition tasks and suggest that illumination effects serve to remove 3D ambiguities.

4.5. Shape versus semantic adaptation in the LOC

A related issue is the selectivity of neuronal activation in high-order object areas to specific shapes versus semantic object categories. It could be argued that the activation in the "different condition" did not attain the maximum because all objects in an epoch belonged to the same category (e.g., faces). In a previous study (Grill-Spector et al., 1999), we compared the activation evoked by different images taken from the same semantic class (dogs) to the activation elicited by images of various objects from different semantic categories. Overall, there was no apparent adaptation effect when different object shapes were limited to the same semantic category. Since LOC is a large region, we examined whether there were sub-regions that nevertheless displayed a reduction in activation when exemplars of the same semantic category were presented. This analysis revealed a small population of such voxels ($4.8 \pm 4.5\%$, S.D. of the entire LOC). However, they were quite variable between subjects both in their extent and in their anatomical location within the LOC. Thus, repetition of

images belonging to the same object class does not produce adaptation in the LOC, but the repetition of an identical shape (object) does produce adaptation.

4.6. Event-related adaptation

So far, the fMR-A results we have discussed stem from block-designed experiments. One difficulty with interpreting the results of block-designed experiments is that the observers may change their cognitive and attentional strategies across and within blocks. This is problematic because attentional modulation has been shown to enhance or attenuate activation in various visual areas (Brefczynski & DeYoe, 1999; Corbetta, Miezin, Dobmeyer, Shulman, & Petersen, 1991; Culham et al., 1998; O'Craven, Rosen, Kwong, Treisman, & Savoy, 1997; Somers, Dale, Seiffert, & Tootell, 1999; Tootell et al., 1998; Wojciulik, Kanwisher, & Driver, 1998). Event-related designs with intermixed trials from different conditions provide a possible solution to this problem (see also Op de Beeck et al., 2001). The use of rapid presentation event-related fMRI paradigms (Buckner et al., 1998) is promising in that it will enable to directly investigate the relationship between differences in brain activation measured by fMRI and behavioral changes that are associated with image repetition.

Application of rapid presentation event-related fMRI to adaptation studies proceeds in the following manner: in each trial, two images are presented in rapid succession, the two images can be either identical, different or the same object that underwent a change. It has been demonstrated (Dale & Buckner, 1997) that responses to trials presented every 2 s add roughly linearly, and can be separated using signal averaging of trial types. Trial types should be counterbalanced within and between scans. Counterbalancing is important in this design because of the overlap of the hemodynamic response of adjacent trials – trials can be spaced as close as 2 s apart but the hemodynamic response lasts approximately 10–16 s. By systematically changing the positions of trials within and across runs the average "trial history" preceding and following a given trial will be equivalent for all trial types. Indeed, a recent study (Kourtzi & Kanwisher, 2000) has used this paradigm to show that changes in object format (line drawing versus gray level) cause fMR-A, indicating the neurons within these regions are invariant to object format.

The use of event-related fMR-A can be also applied to study the tuning curves of a population of neurons, by performing parametric experiments. For example, in the current study, we tested rotation invariance using blocks of images rotated in the range of $-90°$ to $90°$ around the vertical axis. The results reveal that neurons exhibited a recovery from adaptation for rotation, but the adaptation ratio was consistently smaller than 1. Although we had tested a large range of rotations, some of the images within a block were taken at similar viewing angles, e.g., $40°$ and $50°$, which may be within the tuning range of neurons that are sensitive to orientation. One could envision refining this experiment by using event-related fMR-A. Similar to the current experiment, trials will include pairs of images of the same object taken at different viewing angles. The trials will vary in the difference of orientations between images in a pair. Thus, some pairs will be taken at small offsets in the

viewing angle and other in large offsets. By measuring the recovery from adaptation at different viewpoint offsets, we could measure the orientation tuning of this population of neurons.

4.7. Adaptation as a tool for studying other neuronal properties

The use of fMR-A need not be limited to shape adaptation and invariances in object-selective areas. It could be readily extended to other neuronal systems and modalities in which adaptation is manifested: for example, reports of reduced activation in the left prefrontal cortex due to semantic classification of objects (Buckner & Koutstaal, 1998; Wagner, Desmond, Demb, & Glover, 1997) habituation effects in the amygdala (Breiter et al., 1996) or adaptation in the motor cortex (Karni et al., 1995).

We list below a few conjectural examples for uses of fMR-A in other modalities. In studying the representation of vocabulary in language areas, one might hypothesize that words with the same meaning are represented by the same neurons within language areas. Using fMR-A we can compare the activation elicited by identical words to synonyms, or to words that sound the same but have a different meanings, or to different words. In purely semantic representations, we would expect to measure fMR-A by identical words and synonyms, but a recovery from adaptation for words that sound the same and have a different meaning and also for different words (see also Humphreys & Price, 2001; Munhall, 2001).

In motor cortex, one can map putative regions in which the representation of the same motor task is dependent or independent on the hand that performs the task. One would then compare the activation elicited by performing the same motor task with the same hand, the same motor task performed by different hands, and different motor tasks performed by the same hand (see also Parsons, 2001).

Thus, by manipulating experimental parameters and testing recovery from adaptation it should be possible to gain insight into the functional properties of cortical neurons which are beyond the spatial resolution limits imposed by fMRI.

5. Conclusions

We have shown that fMR-A can provide a powerful tool for assessing the functional properties of cortical neurons beyond the spatial resolution of several mm imposed by conventional fMRI. This method enables to tag specific neuronal populations within an area and investigate their functional properties. In the present experiments, we first characterized visual fMR-A in terms of its anatomical localization and duration in the human visual cortex. We then used fMR-A to investigate invariances of object representation in the LOC. Our results show that neurons within LOC are less sensitive to changes in stimulus size and position compared to changes induced by illumination and viewpoint. Moreover, subdivisions within the LOC exhibited different adaptation profiles: an anterior-ventral portion located in the pFs showed a higher level of translation and size invariant

adaptation (indicating a higher degree of invariance) compared to the posterior subdivision (LO).

Acknowledgements

This study was funded by ISF grant 131/97. We thank Y. Moses for providing the face database, and E. Sali and A. Zeira, for providing the car database. We thank E. Okon for technical help and advice, M. Harel for brain surface reconstruction, and T. Hendler, G. Avidan-Carmel, and three anonymous reviewers for helpful comments on the manuscript.

References

Bar, M., Schacher, D., Dale, A. M., & Tootell, R. B. H. (1999). *Society of Neurosciences Abstract*, *25*, 529.

Biederman, I. (1987). Recognition by components: a theory of human image understanding. *Psychological Reviews*, *94*, 115–147.

Booth, M. C., & Rolls, E. T. (1998). View-invariant representations of familiar objects by neurons in the inferior temporal visual cortex. *Cerebral Cortex*, *8*, 510–523.

Boynton, G. M., Engel, S. A., Glover, G. H., & Heeger, D. J. (1996). Linear systems analysis of functional magnetic resonance imaging in human V1. *Journal of Neuroscience*, *16*, 4207–4221.

Brefczynski, J. A., & DeYoe, E. A. (1999). A physiological correlate of the 'spotlight' of visual attention. *Nature Neuroscience*, *2*, 370–374.

Breiter, H. C., Etcoff, N. L., Whalen, P. J., Kennedy, W. A., Rauch, S. L., Buckner, R. L., Strauss, M. M., Hyman, S. E., & Rosen, B. R. (1996). Response and habituation of the human amygdala during visual processing of facial expression. *Neuron*, *17*, 875–887.

Buckner, R. L., Goodman, J., Burock, M., Rotte, M., Koutstaal, W., Schacter, D., Rosen, B., & Dale, A. M. (1998). Functional-anatomic correlates of object priming in humans revealed by rapid presentation event-related fMRI. *Neuron*, *20*, 285–296.

Buckner, R. L., & Koutstaal, W. (1998). Functional neuroimaging studies of encoding, priming, and explicit memory retrieval. *Proceedings National Academy of Science USA*, *95*, 891–898.

Buckner, R. L., Petersen, S. E., Ojemann, J. G., Miezin, F. M., Squire, L. R., & Raichle, M. E. (1995). Functional anatomical studies of explicit and implicit memory retrieval tasks. *Journal of Neuroscience*, *15*, 12–29.

Cheng, K., Waggoner, R., & Tanaka, K. (1999). Patterns of human ocular dominance columns as revealed by high field (4T) functional magnetic resonance imaging. *Society for Neuroscience Abstracts*, *24*, 1422.

Cooper, E. E., Biederman, I., & Hummel, J. E. (1992). Metric invariance in object recognition: a review and further evidence. *Canadian Journal of Psychology*, *46*, 191–214.

Corbetta, M., Miezin, F. M., Dobmeyer, S., Shulman, G. L., & Petersen, S. E. (1991). Selective and divided attention during visual discrimination of shape, color and speed: functional anatomy by positron emission tomography. *Journal of Neuroscience*, *11*, 2383–2402.

Culham, J. C., Brandt, S. A., Cavanagh, P., Kanwisher, N. G., Dale, A. M., & Tootell, R. B. (1998). Cortical fMRI activation produced by attentive tracking of moving targets. *Journal of Neurophysiology*, *80*, 2657–2670.

Dale, A. M., & Buckner, R. L. (1997). Selective averaging of rapidly presented individual trials using fMRI. *Human Brain Mapping*, *5*, 329–340.

Damasio, A. R. (1990). Category-related recognition defects as a clue to the neural substrates of knowledge. *Trends in Neuroscience*, *13*, 95–98.

Damasio, A. R., Tranel, D., & Damasio, H. (1990). Face agnosia and the neural substrates of memory. *Annual Reviews Neuroscience*, *13*, 89–109.

De Gelder, B., & Rouw, R. (2001). Beyond localisation: a dual route account of face recognition. *Acta Psychologica*, *107*, 163–207.

Desimone, R. (1996). Neural mechanisms for visual memory and their role in attention. *The Proceedings of the National Academy of Sciences*, *93*, 13494–13499.

DeYoe, E. A., Bandettini, P., Neitz, J., Miller, D., & Winans, P. (1994). Functional magnetic resonance imaging (FMRI) of the human brain. *Journal of Neuroscience Methods*, *54*, 171–187.

DeYoe, E. A., Carman, G. J., Bandettini, P., Glickman, S., Wieser, J., Cox, R., Miller, D., & Neitz, J. (1996). Mapping striate and extrastriate visual areas in human cerebral cortex. *The Proceedings of the National Academy of Sciences*, *93*, 2382–2386.

Dill, M., & Edelman, S. (1997). Translation invariance in object recognition and its relation to other visual transformations. *Artificial intelligence Memo No. 1610*. Cambridge, MA: MIT AI lab.

Edelman, S. (1998). Computational theories of object recognition. *Trends in Cognitive Sciences*, *1*, 296–304.

Edelman, S., & Duvdevani-Bar, S. (1997). A model of visual recognition and categorization. *Philosophical Transactions of the Royal Society of London B Biological Sciences*, *352*, 1191–1202.

Engel, S. A., Glover, G. H., & Wandell, B. A. (1997). Retinotopic organization in human visual cortex and the spatial precision of functional MRI. *Cerebral Cortex*, *7*, 181–192.

Engel, S. A., Rumelhart, D. E., Wandell, B. A., Lee, A. T., Glover, G. H., Chichilnisky, E. J., & Shadlen, M. N. (1994). fMRI of human visual cortex. *Nature*, *369*, 525–525.

Farah, M. J., Klein, K. L., & Levinson, K. L. (1995). Face perception and within-category discrimination in prosopagnosia. *Neuropsychologia*, *33*, 661–674.

Farah, M. J., Wilson, K. D., Drain, M., & Tanaka, J. N. (1998). What is special about face perception? *Psychological Review*, *105*, 482–498.

Fiser, J., & Biederman, I. (1995). Size invariance in visual object priming of gray-scale images. *Perception*, *24*, 741–748.

George, N., Dolan, R. J., Fink, G. R., Baylis, G. C., Russell, C., & Driver, J. (1999). Contrast polarity and face recognition in the human fusiform gyrus. *Nature Neuroscience*, *2*, 574–580.

Grill-Spector, K., Kushnir, T., Edelman, S., Avidan-Carmel, G., Itzchak, Y., & Malach, R. (1999). Differential processing of objects under various viewing conditions in the human lateral occipital complex. *Neuron*, *24*, 187–203.

Grill-Spector, K., Kushnir, T., Edelman, S., Itzchak, Y., & Malach, R. (1998b). Cue-invariant activation in object-related areas of the human occipital lobe. *Neuron*, *21*, 191–202.

Grill-Spector, K., Kushnir, T., Hendler, T., Edelman, S., Itzchak, Y., & Malach, R. (1998a). A sequence of object processing stages revealed by fMRI in the human occipital lobe. *Human Brain Mapping*, *6*, 316–328.

Grill-Spector, K., Kushnir, T., Hendler, T., & Malach, R. (2000). The dynamics of object-selective correlate with recognition performance in humans. *Nature Neuroscience*, *3*, 837–843.

Gross, C. G., Rocha, M. C., & Bender, D. B. (1972). Visual properties of neurons in inferotemporal cortex of the Macaque. *Journal of Neurophysiology*, *35*, 96–111.

Hadjikhani, N., Liu, A. K., Dale, A. M., Cavanagh, P., & Tootell, R. B. (1998). Retinotopy and color sensitivity in human visual cortical area V8. *Nature Neuroscience*, *1*, 235–241.

Halgren, E., Dale, A. M., Sereno, M. I., Tootell, R. B., Marinkovic, K., & Rosen, B. R. (1999). Location of human face-selective cortex with respect to retinotopic areas. *Human Brain Mapping*, *7*, 29–37.

Hasselmo, M. E., Rolls, E. T., Baylis, G. C., & Nalwa, V. (1989). Object-centered encoding by face-selective neurons in the cortex in the superior temporal sulcus of the monkey. *Experimental Brain Research*, *75*, 417–429.

Henson, R., Shallice, T., & Dolan, R. (2000). Neuroimaging evidence for dissociable forms of repetition priming. *Science*, *287*, 1269–1272.

Humphreys, G. W., & Price, C. (2001). Cognitive neuropsychology and functional brain imaging: implications for functional and anatomical models of cognition. *Acta Psychologica*, *107*, 119–153.

Ito, M., Fujita, I., Tamura, H., & Tanaka, K. (1994). Processing of contrast polarity of visual images in inferotemporal cortex of the macaque monkey. *Cerebral Cortex*, *4*, 499–508.

Ito, M., Tamura, H., Fujita, I., & Tanaka, K. (1995). Size and position invariance of neuronal responses in monkey inferotemporal cortex. *Journal of Neurophysiology*, *73*, 218–226.

James, T. W., Humphrey, G. K., Gati, J. S., Menon, R. S., & Goodale, M. A. (1999). Repetition priming and the time course of object recognition: an fMRI study. *Neuroreport*, *10*, 1019–1023.

Jiang, Y., Haxby, J. V., Martin, A., Ungerleider, L. G., & Parasuraman, R. (2000). Complementary neural mechanisms for tracking items in human working memory. *Science*, *287*, 643–646.

Kanwisher, N. G., McDermott, J., & Chun, M. M. (1997). The fusiform face area: A module in human extrastriate cortex specialized for face perception. *Journal of Neuroscience*, *17*, 4302–4311.

Karni, A., Meyer, G., Jezzard, P., Adams, M. M., Turner, R., & Ungerleider, L. G. (1995). Functional MRI evidence for adult motor cortex plasticity during motor skill learning. *Nature*, *377*, 155–158.

Kim, D, Duong, T. Q., & Kim, S. (2000). High resolution mapping of iso-orientation columns by fMRI. *Nature Neuroscience*, *3*, 164–169.

Kourtzi, Z., & Kanwisher, N. G. (2000). Cortical regions involved in perceiving object shape. *Journal of Neuroscience*, *20*, 3310–3318.

Lehky, S. R., & Sejnowski, T. J. (1988). Network model of shape-from-shading: Neural function arises from both receptive and projective fields. *Nature*, *333*, 452–454.

Li, L., Miller, E. K., & Desimone, R. (1993). The representation of stimulus familiarity in anterior inferior temporal cortex. *Journal of Neurophysiology*, *69*, 1918–1929.

Logothetis, N. K., Pauls, J., & Poggio, T. (1995). Shape representation in the inferior temporal cortex of monkeys. *Current Biology*, *5*, 552–563.

Lueschow, A., Miller, E. K., & Desimone, R. (1994). Inferior temporal mechanisms for invariant object recognition. *Cerebral Cortex*, *4*, 523–531.

Malach, R., Reppas, J. B., Benson, R. R., Kwong, K. K., Jiang, H., Kennedy, W. A., Ledden, P. J., Brady, T. J., Rosen, B. R., & Tootell, R. B. (1995). Object-related activity revealed by functional magnetic resonance imaging in human occipital cortex. *The Proceedings of the National Academy of Sciences*, *92*, 8135–8139.

Martin, A., Lalonde, F. M., Wiggs, C. L., Weisberg, J., Ungerleider, L. G., & Haxby, J. V. (1995). Repeated presentation of objects reduces activity in ventral occipitotemporal cortex: an FMRI study of repetition priming. *Society for Neuroscience Abstracts*, *21*, 1497.

Menon, R. S., Ogawa, S., Strupp, J. P., & Ugurbil, K. (1997). Ocular dominance in human V1 demonstrated by functional magnetic resonance imaging. *Journal of Neurophysiology*, *77*, 2780–2787.

Miller, E. K., Li, L., & Desimone, R. (1991). A neural mechanism for working and recognition memory in inferior temporal cortex. *Science*, *254*, 1377–1379.

Moses, Y., Adini, Y., Ullman, S. (1994). Face recognition: the problem of compensating for illumination changes. *Proceedings of the European Conference on Computer Vision* pp. 286–296.

Muller, J. R., Metha, A. B., Krauskopf, J., & Lennie, P. (1999). Rapid adaptation in visual cortex to the structure of images. *Science*, *285*, 1405–1408.

Munhall, K. G. (2001). Functional imaging during speech production. *Acta Psychologica*, *107*, 95–117.

O'Craven, K. M., Rosen, B. R., Kwong, K. K., Treisman, A., & Savoy, R. L. (1997). Voluntary attention modulates fMRI activity in human MT-MST. *Neuron*, *18*, 591–598.

Ohzawa, I., Sclar, G., & Freeman, R. D. (1985). Contrast gain control in the cat's visual system. *Journal of Neurophysiology*, *54*, 651–667.

Op de Beeck, H., Wagemans, J., & Vogels, R. (2001). Can neuroimaging really tell us what the human brain is doing? The relevance of indirect measures of population activity. *Acta Psychologica*, *107*, 323–351.

Parsons, L. (2001). Integrating cognitive psychology, neurology, and neuroimaging. *Acta Psychologica*, *107*, 155–181.

Perrett, D. I., Smith, P. A. J., Potter, D. D., Mistlin, A. J., Head, A. S., Milner, A. D., & Jeeves, M. A. (1985). Visual cells in the temporal cortex sensitive to face view and gaze direction. *Proceedings of the Royal Society London B*, *223*, 293–317.

Poggio, T., & Edelman, S. (1990). A network that learns to recognize three-dimensional objects. *Nature*, *343*, 263–266.

Puce, A., Allison, T., & McCarthy, G. (1999). Electrophysiological studies of human face perception effects of top–down processing. III: on face-specific potentials. *Cerebral Cortex*, *9*, 445–458.

Rajapakse, J. C., Kruggel, F., Maisog, J. M., & von Cramon, D. Y. (1998). Modeling hemodynamic response for analysis of functional MRI time-series. *Human Brain Mapping*, *6*, 283–300.

Reyment, R., & Joreskog, K. (1993). *Applied factor analysis in the natural sciences*. Cambridge, MA: Cambridge University Press.

Rolls, E. T., Baylis, G. C., Hasselmo, M. E., & Nalwa, V. (1989). The effect of learning on the face selective responses of neurons in the cortex in the superior temporal sulcus of the monkey. *Experimental Brain Research*, *76*, 153–164.

Rugg, M. D., Soardi, M., & Doyle, M. C. (1995). Modulation of event-related potentials by the repetition of drawings of novel objects. *Brain Research: Cognitive Brain Research*, *3*, 17–24.

Savoy, R. (2001). History and future directions of human brain mapping and functional neuroimaging. *Acta Psychologica*, *107*, 9–42.

Schacter, D. L., & Buckner, R. L. (1998). Priming and the brain. *Neuron*, *20*, 185–195.

Sereno, M. I., Dale, A. M., Reppas, J. B., Kwong, K. K., Belliveau, J. W., Brady, T. J., Rosen, B. R., & Tootell, R. B. (1995). Borders of multiple visual areas in humans revealed by functional magnetic resonance imaging. *Science*, *268*, 889–893.

Sobotka, S., & Ringo, J. L. (1993). Investigation of long-term recognition and association memory in unit responses from inferotemporal cortex. *Experimental Brain Research*, *96*, 28–38.

Somers, D. C., Dale, A. M., Seiffert, A. E., & Tootell, R. B. (1999). Functional MRI reveals spatially specific attentional modulation in human primary visual cortex. *The Proceedings of the National Academy of Sciences*, *96*, 1663–1668.

Stern, C. E., Corkin, S., Gonzalez, R. G., Guimaraes, A. R., Baker, J. R., Jennings, P. J., Carr, C. A., Sugiura, R. M., Vedantham, V., & Rosen, B. R. (1996). The hippocampal formation participates in novel picture encoding: evidence from functional magnetic resonance imaging. *The Proceedings of the National Academy of Sciences*, *93*, 8660–8665.

Talairach, J., & Tournoux, P. (1988). *Co-planar stereotaxic atlas of the human brain*. New York: Thieme Medical Publishers.

Tarr, M. J., Kersten, D., & Bülthoff, H. H. (1998). Why the visual recognition system might encode the effects of illumination. *Vision Research*, *38*, 2259–2276.

Tootell, R. B., Hadjikhani, N., Hall, E. K., Marrett, S., Vanduffel, W., Vaughan, J. T., & Dale, A. M. (1998). The retinotopy of visual spatial attention. *Neuron*, *21*, 1409–1422.

Ullman, S. (1996). *High-level vision*. Cambridge, MA: MIT Press.

Ungerleider, L. G., & Mishkin, M. (1982). Two cortical visual systems. In D. J. Ingle, M. A. Goodale, & R. J. W. Mansfield, *Analysis of visual behavior* (pp. 549–586). Cambridge, MA: MIT.

Wagner, A. D., Desmond, J. E., Demb, J. B., & Glover, G. H. (1997). Semantic priming for verbal and pictorial knowledge; a functional MRI study of left inferior prefrontal cortex. *Journal of Cognitive Neuroscience*, *9*, 714–726.

Wang, G., Tanaka, K., & Tanifuji, M. (1996). Optical imaging of functional organization in the monkey inferotemporal cortex. *Science*, *272*, 1665–1668.

Werblin, F. S. (1973). The control of sensitivity in the retina. *Scientific American*, *228*, 70–79.

Wiggs, C. L., & Martin, A. (1998). Properties and mechanisms of perceptual priming. *Current Opinion in Neurobiology*, *8*, 227–233.

Wojciulik, E., Kanwisher, N. G., & Driver, J. (1998). Covert visual attention modulates face-specific activity in the human fusiform gyrus: fMRI study. *Journal of Neurophysiology*, *79*, 1574–1578.